Published in final edited form as:
DNA Repair (Amst). 2013 January 1; 12(1): 53–62. doi:10.1016/j.dnarep.2012.10.005.

Role of the conserved lysine within the Walker A motif of human DMC1

Deepti Sharma[a,1], **Amanda F. Say**[a,2], **LeAnna L. Ledford**[a], **Ami J. Hughes**[a,3], **Hilarie A. Sehorn**[a], **Donard S. Dwyer**[b], and **Michael G. Sehorn**[a,*]

[a]Department of Genetics and Biochemistry, Clemson University, Clemson, SC 29634, United States

[b]Department of Psychiatry, LSU Health Sciences Center-Shreveport, 1501 Kings Highway, Shreveport, LA 71130, United States

Abstract

During meiosis, the RAD51 recombinase and its meiosis-specific homolog DMC1 mediate DNA strand exchange between homologous chromosomes. The proteins form a right-handed nucleoprotein complex on ssDNA called the presynaptic filament. In an ATP-dependent manner, the presynaptic filament searches for homology to form a physical connection with the homologous chromosome. We constructed two variants of hDMC1 altering the conserved lysine residue of the Walker A motif to arginine ($hDMC1_{K132R}$) or alanine ($hDMC1_{K132A}$). The hDMC1 variants were expressed in *Escherichia coli* and purified to near homogeneity. Both $hDMC1_{K132R}$ and $hDMC1_{K132A}$ variants were devoid of ATP hydrolysis. The $hDMC1_{K132R}$ variant was attenuated for ATP binding that was partially restored by the addition of either ssDNA or calcium. The $hDMC1_{K132R}$ variant was partially capable of homologous DNA pairing and strand exchange in the presence of calcium and protecting DNA from a nuclease, while the $hDMC1_{K132A}$ variant was inactive. These results suggest that the conserved lysine of the Walker A motif in hDMC1 plays a key role in ATP binding. Furthermore, the binding of calcium and ssDNA promotes a conformational change in the ATP binding pocket of hDMC1 that promotes ATP binding. Our results provide evidence that the conserved lysine in the Walker A motif of hDMC1 is critical for ATP binding which is required for presynaptic filament formation.

Keywords

DMC1; Meiotic recombination; DNA strand exchange

*Corresponding author at: Department of Genetics and Biochemistry, Clemson University, 105 Collings Street, Biosystems Research Complex Room 314, Clemson, SC 29634, United States. Tel.: +1 864 656 2572; fax: +1 864 656 0393. MSehorn@Clemson.edu (M.G. Sehorn).
[1]Present address: School of Biological Sciences, Nanyang Technological University, 637551, Singapore.
[2]Present address: Department of Experimental Radiation Oncology University of Texas, MD Anderson Cancer Center, Houston, TX 77030, United States.
[3]Present address: Department of Microbiology & Immunology, Northwestern University, Chicago, IL 60611, United States.

Appendix A. Supplementary data

Supplementary data associated with this article can be found, in the online version, at http://dx.doi.org/10.1016/j.dnarep.2012.10.005.

Conflicts of interest statement

The authors declare that there are no conflicts of interest.

1. Introduction

Meiosis is essential for reproduction in most eukaryotic organisms. Haploid gametes are produced from one round of DNA replication followed by two rounds of cell division. This process is initiated by the introduction of programmed DNA double-strand breaks (DSBs) generated by the Spo11 enzyme throughout the genome [1]. The repair of these DSBs primarily occurs through the meiotic homologous recombination (HR) pathway with the goal of establishing a physical linkage between the homologous chromosomes. Linkage between homologous chromosomes is essential for proper segregation of paired chromosomes at meiotic prophase I. Impaired meiotic HR leads to non-disjunction and results in aneuploid gametes or apoptosis.

DSBs formed during meiosis are processed nucleolytically to produce 3′ ssDNA tails that serve as the site of nucleation for two *Escherichia coli* RecA orthologs, RAD51 and DMC1. RAD51 and DMC1 form right-handed helical nucleoprotein filaments on ssDNA tails known as presynaptic filaments [2-4]. The presynaptic filament invades homologous chromosomes searching for homology. Once homology is found, RAD51 and DMC1 catalyze ATP-dependent homologous DNA pairing and displace the complementary strand forming a D-loop [5,6]. D-loop formation is followed by DNA strand exchange [7,8]. DMC1 is expressed exclusively during meiosis while RAD51 is present in both mitotic and meiotic cells. Knockout of *RAD51*$^{-/-}$ in mice results in embryonic lethality [9,10]. Although *DMC1*$^{-/-}$ knockout mice are viable, they are sterile indicating a role for DMC1 in mammalian meiotic recombination [11].

The exact requirement of DMC1 during meiosis and its distinction from RAD51 is poorly understood. Recent biochemical analyses suggest the functional differences between these two recombinases are attributed to differences in their accessory factors [4]. Despite structural similarities between RAD51 and DMC1 [4] there are biochemical differences between the activities of the two recombinases [5,12-15]. Furthermore, Bugreev et al. [16] provided evidence that D-loops formed by hDMC1 resist dissociation by Rad54. Under similar conditions, D-loops formed by RAD51 readily dissociate [17].

A significant region of homology between RecA, RAD51 and DMC1 is the conserved ATP binding Walker A motif [18,19]. The type A consensus sequence (GXXXXGKT/S) is involved in binding to the phosphate group of ATP [20]. According to previous studies, ATP binding in RecA induces a conformational change that is required for its DNA binding activity [21,22] while ATP hydrolysis is required for filament turnover [23]. ATP binding by hRAD51 is essential for its recombinase activity, whereas variants defective for ATP hydrolysis possess robust homologous DNA pairing and DNA strand exchange activity [24]. There is preliminary evidence that hDMC1-mediated recombination can occur in the absence of ATP hydrolysis [5,12].

In this study, we determine the role of Walker A motif and dissect how ATP binding and hydrolysis affects hDMC1-mediated homologous recombination. With this goal in mind, we constructed two hDMC1 Walker A variants. The conserved Walker lysine residue was changed to arginine or alanine with the expectation of generating variants incapable of binding or hydrolyzing the ATP, respectively. Biochemical analysis of the purified hDMC1 Walker variants reveal that mutation of the conserved lysine within the Walker A motif of hDMC1 affects ATP binding and hydrolysis. Furthermore, hDMC1-mediated recombination requires ATP binding.

2. Experimental procedures

2.1. Plasmids

The cDNA for human *DMC1* was a kind and generous gift from Dr. Patrick Sung. A six-histidine tag was added to the 5′ end of the human *DMC1* cDNA by PCR as described [5]. The PCR product was inserted into the pET11c vector (Novagen) and sequenced to ensure no undesired mutations were present. Quickchange site-directed mutagenesis was performed on the pET11c-hDMC1$_{WT}$ plasmid to change the conserved lysine at position 132 to arginine or alanine. The hDMC1$_{K132R}$ and hDMC1$_{K132A}$ pET11c expression plasmids were sequenced to ensure only the desired mutations were present.

2.2. Expression and purification of hDMC1$_{WT}$, hDMC1$_{K132R}$ and hDMC1$_{K132A}$

The hDMC1$_{WT}$ expression plasmid was introduced into the BLR(DE3) strain of *E. coli*. The cells were grown at 37 °C and protein expression was induced by the addition of IPTG. After the cells were harvested, the cell paste (40 g) was resuspended in Buffer A (50 mM Tris pH 7.5, 1 mM EDTA, 10% sucrose, 0.01% Igepal, 1 mM β-mercaptoethanol, 0.1 mg/mL lysozyme, 1 mM benzamidine, 1 mM PMSF, and protease inhibitors aprotinin, chymostatin, leupeptin, and pepstatin A at a final concentration of 5 μg/mL) containing 250 mM KCl. The subsequent steps were performed at 4 °C. The re-suspended cells were lysed by sonication and the extract was clarified by ultracentrifugation. Ammonium sulfate was added to the clarified lysate and the precipitated protein was subjected to centrifugation, re-suspended in Buffer B (20 mM K_2HPO_4 pH 7.4, 10% glycerol, 1 mM EDTA, 1 mM DTT) and loaded onto a Q Sepharose column. The peak fractions of hDMC1$_{WT}$ were pooled and incubated with 1 mL of Nickel NTA Sepharose (GE Healthcare). The bound protein was eluted with 10 mL of Buffer B containing 500 mM imidazole and 300 mM KCl. The eluate was loaded onto a Mono S column (GE Healthcare). Peak fractions containing hDMC1$_{WT}$ were diluted with Buffer B and loaded onto a Mono Q column (GE Healthcare). The peak fractions containing hDMC1$_{WT}$ were concentrated and stored in small aliquots at −80 °C. The hDMC1$_{K132R}$ and hDMC1$_{K132A}$ proteins were expressed and purified using the procedure as described for hDMC1$_{WT}$. Three independent preparations yielded the same results in the biochemical experiments.

2.3. DNA substrates

The ϕX174 viral (+) strand (ssDNA) and ϕX174 replicative form I (dsDNA) was purchased from New England Biolabs. The ϕX174 replicative form I was digest with ApaLI (New England Biolabs) to linearize the DNA. The supercoiled pBluescript DNA was purified using a commercially available kit (Qiagen). All the oligonucleotides were from Integrated DNA Technology. Oligonucleotides were gel purified on a 10% denaturing polyacrylamide gel in TAE (40 mM Tris-acetate pH 7.5, 0.5 mM EDTA). The DNA was excised from the gel, electroeluted overnight and stored in TE buffer (10 mM Tris–HCl pH 7.5, 0.5 mM EDTA). Oligonucleotides OL83 (5′-TTTATATCCTTTACTTTATTTTCTATGTTTATTCATTTACTTATTTTGTATTATCCTTATACTTATTTACTTTATGTTCATTT-3′) and OL90 (5′-AAATCAATCTAAAGTATATATGAGTAAACTTGGTCTGACAGTTACCAATGCTTAATCAGTGAGGCACCTATCTCAGCGATCTGTCTATT-3′) were 5′-end labeled with [γ-^{32}P]-ATP using T4 polynucleotide kinase. A Micro Bio-Spin 30 Column (Bio-Rad) was used to remove unincorporated [γ-^{32}P] ATP. To generate an 83 bp dsDNA substrate, equimolar amounts oligonucleotide ^{32}P-OL83 and its complement were incubated at 95 °C for 5 min in Buffer C (10 mM Tris–HCl pH 8.0, 10 mM NaCl, 1 mM EDTA) and slowly cooled to room temperature. The annealed DNA substrates were gel purified on 10% non-denaturing polyacrylamide gels. The substrates were excised from the polyacrylamide gel, electroeluted and filter dialyzed as described [25].

2.4. ATPase assay

hDMC1$_{WT}$, hDMC1$_{K132R}$ and hDMC1$_{K132A}$ (3 μM) were incubated with 0.1 mM [γ-^{32}P] ATP in 10 μL reaction mixture with Buffer R (20 mM Tris–HCl pH 7.5, 2.4 mM $MgCl_2$, 50 mM KCl, 1 mM DTT) either in the absence or presence of ssDNA ϕX174 (+) virion DNA (15 μM nucleotides) or linearized ϕX174 replicative form I dsDNA (15 μM base pairs) at 37 °C. At the indicated times, 1.5 μL aliquots were removed and the reaction was stopped by the addition of an equal volume of 0.5 M EDTA. An aliquot of the stopped reaction was applied to polyethyleneimine-cellulose (PEI) plates and subjected to thin layer chromatography. The amount of released ^{32}P and γ-^{32}P ATP was determined using a Typhoon phosphorimager (GE Healthcare).

2.5. φX174 DNA mobility shift assay

Increasing amounts of hDMC1$_{WT}$, hDMC1$_{K132R}$ and hDMC1$_{K132A}$ were incubated with ϕX174 ssDNA (30 μM nucleotides), linearized ϕX174 dsDNA (30 μM base pairs), or both ssDNA and dsDNA for 10 min at 37 °C in 12.5 μL Buffer R containing 100 mM KCl in the presence or absence of 2 mM ATP, ATP-γ-S, AMP–PNP or ADP. DNA loading dye (10 mM Tris–HCl pH 7.5, 0.5 mM EDTA, 50% glycerol, 0.1% Orange G) was added to the reaction and the samples were resolved in 0.9% agarose gels at 6.6 V/cm followed by ethidium bromide staining. Images were captured and analyzed using Quantity One (Bio-Rad) software. A control reaction was deproteinized by treatment with SDS (0.5% final) and Proteinase K (0.5 mg/mL) at 37 °C for 10 min prior to loading in a 0.9% agarose gel.

2.6. Oligonucleotide DNA mobility shift assay

The ^{32}P-labeled OL90 ssDNA (4.5 μM) was incubated with increasing concentrations of hDMC1$_{WT}$, hDMC1$_{K132R}$ and hDMC1$_{K132A}$ for 10 min at 37 °C in 10 μL of Buffer R containing 100 mM KCl in the presence or absence of 2 mM ATP, ATP-γ-S, AMP–PNP, or ADP. DNA loading dye was added to the reaction and the samples were subjected to 12% non-denaturing PAGE at 18.3 V/cm. The gels were dried, analyzed with a phosphorimager and quantified with ImageQuant (GE Healthcare) software. A control reaction was deproteinized by treatment with SDS (0.5% final) and Proteinase K (0.5 mg/mL) at 37 °C for 10 min prior to loading a 12% non-denaturing polyacrylamide gel.

2.7. ATP Binding assay

α-^{32}P-ATP (0.1 mM) was incubated with 10 μM hDMC1$_{WT}$, hDMC1$_{K132R}$ or hDMC1$_{K132A}$ in 60 μL Buffer R containing either 0, 2, or 4 mM $CaCl_2$ in the presence or absence of ϕX174 ssDNA (15 μM nucleotides) for 10 min at 37 °C. An aliquot was applied to a nylon membrane (GE Healthcare) and filtered through a manifold apparatus (Denville Scientific). After 2 washes with Buffer R containing 0, 2 or 4 mM $CaCl_2$ the nylon membrane was dried and analyzed with a phosphorimager to determine the percent nucleotide bound.

2.8. Nuclease protection assay

The ^{32}P-labeled OL90 ssDNA (4.5 μM) was incubated with either 3 μM of hDMC1$_{WT}$, hDMC1$_{K132R}$ or hDMC1$_{K132A}$ for 10 min at 37 °C in Buffer R containing either 0, 2 or 4 mM $CaCl_2$ in the presence or absence of ATP (2 mM). DNase I nuclease (1 unit) was added to the reaction followed by further incubation at 37 °C. An aliquot was withdrawn at different time points, deproteinized by treatment with SDS (0.5% final) and Proteinase K (0.5 mg/mL) at 37 °C for 10 min and subjected to 12% non-denaturing PAGE at 18.3 V/cm. The gels were dried, analyzed with a phosphorimager and quantified with ImageQuant.

2.9. D-loop assay

The ^{32}P-labeled OL90 D-loop substrate (2.5 μM nucleotides) was incubated with 1 μM hDMC1$_{WT}$, hDMC1$_{K132R}$ and hDMC1$_{K132A}$ in Buffer R (final reaction volume 12.5 μL) in the presence or absence of 2 mM ATP, ATP-γ-S, AMP–PNP, or ADP at 37 °C for 2 min followed by the addition of either 2 or 4 mM $CaCl_2$. The reaction was initiated by addition of pBluescript SK replicative form I (35 μM base pairs). Aliquots were withdrawn at various time points, deproteinized by treatment with SDS (0.5% final) and Proteinase K (0.5 mg/mL) at 37 °C for 10 min and subjected to 0.9% agarose gel electrophoresis in TAE buffer at 15 V/cm. The gels were dried, analyzed with a phosphorimager and quantified with ImageQuant.

2.10. DNA Strand exchange assay

The unlabeled OL83 oligonucleotide (10 μM nucleotides) was incubated with either 3 μM hDMC1$_{WT}$, hDMC1$_{K132R}$ or hDMC1$_{K132A}$ for 10 min at 37 °C in 11 μL reaction Buffer R in the presence or absence of ATP. The duplex DNA (5 μM base pairs) composed of ^{32}P-labeled OL83 annealed to its complement was added with 1 μL of 50 mM spermidine to the reaction mixture and further incubated for 45 min at 37 °C (final reaction volume 12.5 μL). Aliquots were withdrawn at various time points, deproteinized by treatment with SDS (0.5% final) and Proteinase K (0.5 mg/mL) at 37 °C for 10 min and subjected to non-denaturing electrophoresis using 12% polyacrylamide gels in TAE buffer at 15 V/cm. The gels were dried, analyzed with a phosphorimager and quantified with ImageQuant.

2.11. Energy minimization

Energy minimization was performed with Accelrys Discovery Studio 3.1. Atomic coordinates for hDMC1 (PDB ID: 1v5w) and *E. coli recA* (PDB ID: 2reb) were obtained from the Protein Data Bank. hDMC1$_{K132R}$ was created by replacing K132 in the hDMC1$_{WT}$ structure with arginine. The hDMC1$_{WT}$ and hDMC1$_{K132R}$ were then subjected to energy minimization using CHARMM22 with 1000 steps of the steepest descent followed by 100,000 steps of the conjugate gradient method. From the minimized structures, measurements were obtained between pairs of atoms in key residues that lie in a putative nucleotide-binding cleft.

3. Results

3.1. Mutation of the conserved lysine in the hDMC1 Walker A motif

The human DMC1 recombinase forms a presynaptic filament and catalyzes homologous DNA pairing and DNA strand exchange in an ATP-dependent manner [5,12]. We constructed a bacterial expression plasmid harboring wild type hDMC1 (hDMC1$_{WT}$) and used site-directed mutagenesis to mutate the conserved Walker A motif lysine residue at position 132 to either arginine (hDMC1$_{K132R}$) or alanine (hDMC1$_{K132A}$, Fig. 1A) in order to define the role of ATP binding and ATP hydrolysis in hDMC1. Previous studies on other ATPase proteins that contain a Walker A motif [24,26-28] demonstrated that substitution of the conserved lysine in the Walker A motif to arginine permits ATP binding but not hydrolysis while an alanine substitution compromises ATP binding. We devised a method based on previous work [5] to purify milligram quantities of hDMC1$_{WT}$, hDMC1$_{K132R}$ and hDMC1$_{K132A}$ variant proteins (Fig. 1B, lanes 1–3, respectively). The wild type and variant hDMC1 proteins were purified using the identical protocol that included ammonium sulfate precipitation, Q-Sepharose, Nickel affinity chromatography, Mono Q and Mono S chromatography [5]. hDMC1$_{WT}$, hDMC1$_{K132R}$ and hDMC1$_{K132A}$ proteins demonstrated the same chromatographic properties. This procedure yielded protein that was greater than 95% pure for hDMC1$_{WT}$, hDMC1$_{K132R}$ and hDMC1$_{K132A}$ proteins. Three independent preparations for each protein yielded similar results in all the biochemical assays.

3.2. hDMC1$_{K132R}$ and hDMC1$_{K132A}$ are defective in ATP hydrolysis

To confirm that the hDMC1$_{K132R}$ and hDMC1$_{K132A}$ variants lacked ATP hydrolysis activity, we used thin layer chromatography [25,29]. ATP hydrolysis activity was monitored in the presence or absence of ssDNA or dsDNA. Consistent with previous reports [5,30,31], the ATP hydrolysis activity of hDMC1$_{WT}$ (k_{cat} = 0.6 min^{-1} was stimulated in the presence of ssDNA (k_{cat} = 2.5 min^{-1}, Fig. 1C). In contrast to human and *Saccharomyces cerevisiae* RAD51 recombinases [6,24], the ATPase activity of hDMC1$_{WT}$ was weakly stimulated by linearized dsDNA (k_{cat} = 0.8 min^{-1}, Fig. 1C). As expected, the hDMC1$_{K132R}$ and hDMC1$_{K132A}$ mutant proteins were unable to hydrolyze ATP regardless of the presence of ssDNA or dsDNA.

3.3. DNA binding of hDMC1$_{WT}$, hDMC1$_{K132R}$ and hDMC1$_{K132A}$ using plasmid length substrates

Published studies [6,13,32] have shown that hRAD51 binds DNA in an ATP-independent manner. To address whether hDMC1 also bound DNA in an ATP dependent manner, we used an electrophoretic DNA mobility shift assay. First, we incubated increasing concentrations of the hDMC1$_{WT}$, hDMC1$_{K132R}$ or hDMC1$_{K132A}$ protein with a mixture of equal amounts of plasmid length ϕX174 ssDNA and linearized ϕX174 dsDNA. As shown in Fig. 2, hDMC1$_{WT}$, hDMC1$_{K132R}$ and hDMC1$_{K132A}$ preferentially bound ssDNA in the presence of ATP, with higher concentrations of each variant of hDMC1 required to completely shift the dsDNA (panel I–III, lanes 2–5). Using the highest concentration of each hDMC1 variant that completely shifted the ssDNA and dsDNA, we substituted ATP in the reaction for either ATP-γ-S, AMP–PNP or ADP (Fig. 2, panel I–III, lanes 6–8, respectively) or removed nucleotide (Fig. 2, panel I–III, lane 9). Fig. 2 shows hDMC1$_{WT}$, hDMC1$_{K132R}$ and hDMC1$_{K132A}$ shifted a similar amount of ssDNA and dsDNA regardless of presence or absence of ATP, ATP-γ-S, AMP–PNP, or ADP.

3.4. DNA binding of hDMC1$_{WT}$, hDMC1$_{K132R}$ and hDMC1$_{K132A}$ using oligonucleotide substrates

The DNA mobility shift assay using plasmid length DNA substrates did not reveal a nucleotide dependence of the DNA binding activity of hDMC1. During the course of our DNA mobility shift experiments, we switched to an oligonucleotide based electrophoretic DNA mobility shift assay. In this assay, increasing concentrations of the hDMC1$_{WT}$, hDMC1$_{K132R}$ or hDMC1$_{K132A}$ were incubated with the 90-base ssDNA substrate and the reactions were resolved on polyacrylamide gels. Our results show that hDMC1$_{WT}$ bound 100% of the ssDNA in the presence of ATP, while the absence of ATP resulted in a shift of only ~60% of the 90-base ssDNA substrate (Fig. 3, panel I, compare lanes 5 and 6). Since presynaptic filament formation of hDMC1 on ssDNA is dependent upon the presence of ATP [5,12,33], we reasoned that the complete shift of ssDNA in the presence of ATP was the result of presynaptic filament formation, whereas a DNA shift of ~60% was due to formation of stacked rings of hDMC1 on ssDNA [5,12,33]. We used this property of hDMC1 to examine the nucleotide dependence of nucleoprotein filament formation of the hDMC1$_{K132R}$ and hDMC1$_{K132A}$ proteins. As shown in Fig. 3, incubation of increasing concentrations of hDMC1$_{K132R}$ (panel II, lanes 2–5) and hDMC1$_{K132A}$ (panel III, lanes 2–5) in the presence of ATP resulted in approximately ~55–65% shift of ssDNA similar to that seen in the absence of ATP (panel II and III, lane 6). These results suggested hDMC1$_{K132R}$ and hDMC1$_{K132A}$ formed stacked rings on the ssDNA in the presence of ATP.

We examined whether substitution of ATP-γ-S or AMP–PNP in place of ATP resulted in a complete shift of the ssDNA by hDMC1. In the presence of ATP-γ-S, the hDMC1$_{WT}$, hDMC1$_{K132R}$ and hDMC1$_{K132A}$ proteins were unable to completely shift the ssDNA (Fig. 3, panel I–III, lane 11) suggesting ATP-γ-S does not support presynaptic filament formation

of hDMC1. The substitution of AMP–PNP facilitated a complete shift of the ssDNA with $hDMC1_{WT}$ but not for $hDMC1_{K132R}$ and $hDMC1_{K132A}$ (Fig. 3, panel I–III, lane 14). A previous report showed that calcium stabilized the hDMC1-ATP complex [12]. Addition of calcium at two different concentrations resulted in a shift of ~84–88% of the ssDNA in the presence of ATP by $hDMC1_{K132R}$ (Fig. 3 panel II, lanes 7 and 8) while no appreciable increase in the DNA shift occurred with $hDMC1_{K132A}$ under any condition tested (Fig. 3, panel III).

3.5. ATP binding of $hDMC1_{WT}$, $hDMC1_{K132R}$ and $hDMC1_{K132A}$

The finding that $hDMC1_{K132R}$ was capable of shifting more ssDNA in the presence of ATP when calcium was present suggested to us that the $hDMC1_{K132R}$ not only lacked ATP hydrolysis but was also compromised in its ability to bind ATP. To determine whether the $hDMC1_{K132R}$ protein had reduced affinity for ATP, we performed a filter-binding assay [12]. In this assay, the hDMC1 protein was incubated with α–^{32}P-ATP in the absence or presence of calcium and/or ssDNA. As shown in Fig. 4A, $hDMC1_{WT}$ retained ~57% of the bound nucleotide in the absence of ssDNA (lane 2). As we suspected, $hDMC1_{K132R}$ was unable to retain nucleotide in the absence of ssDNA, Fig. 4A (lane 3). A small increase in the amount of bound ATP by $hDMC1_{K132R}$ was observed when ssDNA was incorporated into the reaction (Fig. 4A, lane 6).

We examined whether calcium would stabilize a complex of ATP [12] with each hDMC1 variant by using two different concentrations of calcium. In the absence of ssDNA, addition of calcium significantly increased the amount of bound ATP with $hDMC1_{WT}$ (Fig. 4, compare Panel A lane 2 with Panel B and C lane 2) with only a small increase in bound ATP with $hDMC1_{K132R}$ (Fig. 4, Compare Panel A lane 3 with Panel B and C lane 3). When $hDMC1_{WT}$ was incubated with calcium and ssDNA, the amount of bound ATP increased ~2 fold (Fig. 4, Compare Panel A lane 5 with Panel B and C lane 5). $hDMC1_{K132R}$ bound a higher amount of the ATP when calcium and ssDNA were present (Fig. 4, Compare Panel A lane 6 with Panels B and C lane 6) albeit at significantly reduced levels compared to $hDMC1_{WT}$. $hDMC1_{K132A}$ was unable to bind ATP regardless of the presence of calcium and/or ssDNA. It is important to note that ssDNA stimulates the rate of ATP hydrolysis of $hDMC1_{WT}$, however at the time points used in these experiments we expected only 5–6% of the ATP to be hydrolyzed by $hDMC1_{WT}$ in the absence of calcium. The presence of calcium inhibits the hydrolysis of ATP by hDMC1 [12]. Taken together, these results indicate the $hDMC1_{K132R}$ possesses reduced affinity for ATP that can be partially restored by the addition of calcium and presence of ssDNA.

3.6. Presynaptic filament formation by $hDMC1_{WT}$, $hDMC1_{K132R}$ and $hDMC1_{K132A}$

Since hDMC1 binds ssDNA as stacked rings in the absence of ATP [5,12,33] and nucleoprotein filaments in the presence of ATP [5,12], we surmised that the incomplete shift of ssDNA in the oligonucleotide binding assay was due to the presence of stacked rings of hDMC1. To determine whether hDMC1 formed presynaptic filaments on the ssDNA a nuclease protection assay was used [24,34]. We first confirmed that DNase I digestion of the ssDNA substrate was not affected by the presence of calcium (Fig. 5A). The $hDMC1_{WT}$ protein was incubated with ssDNA in the presence of ATP with or without 2 and 4 mM calcium. After a brief incubation, DNase I was added to the reaction. The time course of the DNase I digestion shows that $hDMC1_{WT}$ in the presence of ATP (Fig. 5B, WT, lanes 1–5), 2 mM and 4 mM calcium (Fig. 5B, lanes 7–11 and 13–17, respectively) completely protected the ssDNA from DNase I digestion during the course of the 30 min reaction. In the absence of ATP, the $hDMC1_{WT}$ protein was unable to protect the ssDNA from DNase I (Fig. 5, panel B, WT, lanes 6, 12 and 18), regardless of the presence of calcium. The $hDMC1_{K132R}$ briefly delayed DNase I digestion of the ssDNA substrate in the presence of

calcium with slightly higher concentrations of calcium (4 mM) providing greater protection (Fig. 5B, K132R). Calcium did not afford protection to ssDNA in the presence of $hDMC1_{K132A}$ (Fig. 5B, K132A). We interpret protection of the ssDNA in the presence of ATP to result from the formation of a presynaptic filament, while digestion of the ssDNA in the absence of ATP resulted from stacked DMC1 rings on ssDNA. These results suggested the $hDMC1_{K132R}$ protein formed partial presynaptic filaments but only when both ATP and 4 mM calcium were present.

3.7. D-loop formation by $hDMC1_{WT}$, $hDMC1_{K132R}$ and $hDMC1_{K132A}$

The results from the above experiments confirm previous findings [5,12] that ATP binding is required for presynaptic filament formation. To determine whether hDMC1-mediated DNA homologous pairing was dependent upon nucleotide binding or hydrolysis, we used an assay that measured the formation of a D-loop. In this assay, the radiolabeled oligonucleotide is assimilated into a supercoiled duplex DNA through base pairing with a region of complementary sequence within the duplex DNA. As a result, the homologous sequence is displaced forming a D-loop (Fig. 6A). We show $hDMC1_{WT}$ catalyzes the formation of a D-loop in the presence of magnesium and ATP or AMP–PNP (Fig. 6B, panel I, [5,12]). In agreement with previous studies [12], calcium stimulated D-loop formation by $hDMC1_{WT}$ in the presence of ATP and to a lesser extent, AMP–PNP. Maximal D-loop formation by $hDMC1_{WT}$ required ATP and not AMP–PNP regardless of the presence (Fig. 6B, compare lanes 4 and 12) or absence of calcium (Fig. 6B, compare lanes 7 and 13). Considering the reduced affinity of $hDMC1_{K132R}$ for ATP and the unstable presynaptic filaments formed by $hDMC1_{K132R}$, we wished to determine whether the $hDMC1_{K132R}$ presynaptic filament was functionally capable of homologous DNA pairing. As shown in Fig. 6, very weak D-loop formation by $hDMC1_{K132R}$ (~1%) was detected in the presence of ATP and calcium (Fig. 6B, panel II and panel III) whereas $hDMC1_{K132A}$ was unable to form D-loops under any conditions tested (Supp. Fig. 1).

3.8. DNA strand exchange by $hDMC1_{WT}$, $hDMC1_{K132R}$ and $hDMC1_{K132A}$

The weak D-loop formation activity of $hDMC1_{K132R}$ led us to use an oligonucleotide-based DNA homologous pairing and strand exchange assay [35]. Here, hDMC1 was incubated first with an oligonucleotide ssDNA substrate in the presence of ATP to allow presynaptic filament formation followed by addition of radiolabeled dsDNA to initiate the reaction. DNA strand exchange is detected when the radiolabeled strand of the dsDNA substrate is replaced by the unlabeled ssDNA within the presynaptic filament. The radiolabeled reaction products are separated on a polyacrylamide gel. In agreement with published work, hDMC1 catalyzed DNA strand exchange in an ATP dependent manner that was stimulated by the addition of calcium (Fig. 7B, [12]. The addition of 4 mM calcium was inhibitory to $hDMC1_{WT}$ reducing the amount of strand exchange product 8 fold. Interestingly, $hDMC1_{K132R}$ yielded ~12% DNA strand exchange that was dependent upon the presence of 4 mM calcium (Fig. 7C) that inhibited the DNA strand exchange activity of $hDMC1_{WT}$ (Fig. 7, panel B, lane 15). Furthermore, $hDMC1_{K132R}$ was unable to commence DNA strand exchange at the lower concentration of calcium (2 mM, Fig. 7C, lane 15) found to be optimal for $hDMC1_{WT}$ DNA strand exchange activity. In all conditions tested, $hDMC1_{K132A}$ was unable to promote DNA strand exchange (Supp. Fig. 2). These results indicate that the $hDMC1_{K132R}$ protein retains DNA strand exchange activity dependent upon the presence of calcium and ATP.

3.9. Molecular modeling of the ATP binding pocket of $hDMC1_{K132R}$

Energy minimization was performed on the ribbon regions of $hDMC1_{WT}$ and $hDMC1_{K132R}$. This analysis revealed a significant compaction of the putative nucleotide-binding site in $hDMC1_{K132R}$ relative to that of the $hDMC1_{WT}$. The hDMC1 residues (Fig. 8A and B)

correspond to their counterparts in the *recA* protein crystallized with ADP present (Fig. 8C, [20]). In $hDMC1_{WT}$ (Fig. 8A), the loop containing R129 and K132 is extended straight outward from the helix and the distance between R129 and E162 (which defines the width of the putative binding cleft) is 4.15 Å. In $hDMC1_{K132R}$ (Fig. 8B), this same loop is displaced upwards and the distance between R129 and E162 is 3.6 Å. Moreover, the length of the binding pocket has decreased from 17.45 Å in $hDMC1_{WT}$ to 14.03 Å in $hDMC1_{K132R}$ (Fig. 8). Part of the driving force for the changes in this loop may be stronger **π**–cation interactions between F128 and R132 than with K132. Furthermore, R132 has greater potential for hydrogen bonding with main chain O atoms of residues 126–128 than K132. These additional hydrogen bonds may alter the flexibility of this critical loop. As a result of these and other changes, the putative binding pocket may be too narrow or short to readily accept ATP, thus reducing binding affinity.

4. Discussion

In this study, Walker A motif variants of hDMC1 and nucleotide analogs were used to examine the role of ATP binding and hydrolysis in hDMC1-mediated homologous recombination.

We constructed $hDMC1_{K132R}$ and $hDMC1_{K132A}$ by substituting the conserved lysine in the Walker A motif to either arginine or alanine. The expectation was the $hDMC1_{K132R}$ and $hDMC1_{K132A}$ variants would fail to hydrolyze or bind ATP, respectively [21,24,26,28].

In agreement with previous studies, we found $hDMC1_{WT}$ ATP hydrolysis activity was stimulated by the presence of ssDNA [30,31,36] as shown for RecA [37] and RAD51 [24]. As expected, neither $hDMC1_{K132R}$ nor $hDMC1_{K132A}$ retained ATP hydrolysis activity. Interestingly, our results showed that unlike RAD51 [6,24], the ATP hydrolysis activity of $hDMC1_{WT}$ was only weakly stimulated by dsDNA (0.8 min^{-1}). Given ATP hydrolysis is linked with disassembly of RecA presynaptic filaments [38], it is possible the weak stimulation of $hDMC1_{WT}$ ATP hydrolysis by dsDNA allows for longer and presumably more stable filament formation on dsDNA [4].

The results from the DNA mobility shift assay that utilized plasmid length ssDNA and linearized dsDNA yielded results similar to those reported for hRAD51 [24], indicating a lack of dependence on the presence of nucleotide. However, when short oligonucleotide substrates were incubated with hDMC1 in the DNA mobility shift assays, two modes of ssDNA binding were observed. In the presence of ATP or AMP–PNP, $hDMC1_{WT}$ completely bound the oligonucleotide ssDNA substrate shifting all the substrate to the well of the gel. These reaction conditions were previously reported to support nucleoprotein filament formation by hDMC1 [5]. The hDMC1 nucleoprotein filament binds DNA in an extend conformation [4] which may give rise to the hDMC1–ssDNA complex trapped in the well of the polyacrylamide gel. However, we cannot rule out the possibility that hDMC1 forms networks that are trapped in the well of the gel. Contrastingly, when $hDMC1_{WT}$ was incubated in the absence of nucleotide, only a partial shift of the oligonucleotide ssDNA substrate was observed. Previous work demonstrated the absence of nucleotide resulted in stacked rings of hDMC1 on ssDNA [5,12,33]. The partial shift of the ssDNA substrate by hDMC1 in the absence of ATP suggested the interaction between the ssDNA and the stacked rings of hDMC1 was transient, potentially leaving regions of the ssDNA unbound. In support of this idea, DNase I rapidly digested ssDNA bound by hDMC1 in the absence of ATP. In contrast, the ssDNA substrate was protected from DNase I digestion by hDMC1 presynaptic filaments formed in the presence of ATP.

Considering the substitution of arginine for the conserved lysine within the Walker A motif of hDMC1 was expected to permit binding but not hydrolysis of ATP [21,24,26,28], we

were surprised $hDMC1_{K132R}$ failed to completely shift the ssDNA in the DNA mobility shift assay in the presence of ATP or AMP–PNP as seen with $hDMC1_{WT}$. Our ATP binding experiments revealed substitution of the conserved lysine to arginine resulted in a significantly reduced ability of $hDMC1_{K132R}$ to bind ATP. As a result, $hDMC1_{K132R}$ was compromised in the ability to form stable presynaptic filaments capable of protecting ssDNA in the nuclease protection assay. The $hDMC1_{K132R}$ presynaptic filaments that did form required calcium to commence homologous DNA pairing and DNA strand exchange albeit very weakly. Taken together, our results showed that hDMC1 requires ATP binding to commence DNA homologous pairing and DNA strand exchange. Although the activity seen with $hDMC1_{K132R}$ was weak, it is in agreement with other recombinases [24,27,28,39].

Structural studies of hDMC1 [40,41] showed different conformations of the ATP binding pocket when hDMC1 is bound to ssDNA. In agreement with these studies, the presence of ssDNA increased the amount of ATP bound by $hDMC1_{K132R}$, suggesting the conformation of the ATP pocket changed to accommodate the nucleotide upon binding DNA. Similarly, the addition of calcium increased the amount of nucleotide bound by the $hDMC1_{K132R}$ (~10%). These results are consistent with previous reports demonstrating calcium inhibited ATP hydrolysis to stabilize the hDMC1-ssDNA presynaptic filament [12]. Furthermore, crystal structures of eukaryotic and archeal RAD51 family members showed the ATP hydrolysis site to be located at the interface between monomers of the nucleoprotein filament. The X-ray crystal structure of RecA–ADP complex indicate the conserved lysine residue in the P-loop interacts with the β and γ phosphates of ATP [20]. The substitution of the conserved lysine in the Walker A motif to an alanine removes the positive charge resulting in the expected loss of ATP binding; however, the substitution of lysine for arginine retains the positive charge. Our energy minimization of $hDMC1_{K132R}$ suggests the substitution of lysine with the bulky side chain of arginine changes the ATP binding pocket resulting in a significant drop in affinity for ATP. Interestingly, AMP–PNP did not substitute for ATP in presynaptic filament formation by $hDMC1_{K132R}$ even with the addition of calcium as in the case with $hDMC1_{WT}$. The substitution of arginine likely altered the conformation of the ATP binding pocket such that AMP–PNP was sterically impeded. The results strongly suggest the lysine residue at position 132 is directly involved in the binding and alignment of ATP.

When ssDNA, calcium or both ssDNA and calcium were included in the nucleotide binding reaction, the amount of nucleotide retained by $hDMC1_{K132R}$ increased. Previous studies revealed that DNA binding induced conformational changes in RecA [42]. Based on these observations, we propose that binding of ssDNA and calcium each induce a conformational change in the hDMC1 that stabilizes bound ATP. The site of calcium binding in hDMC1 is unknown. One explanation first proposed by Bugreev et al. [12] was that the calcium ion binds to a site different than the ATPase pocket to induce a conformational change within the ATP binding pocket of hDMC1 that stabilizes the presynaptic filament. However, the possibility remains that the calcium ion binds within the ATP binding pocket to align ATP for binding. In HR reactions, accessory proteins including the Hop2–Mnd1 complex and presumably the Sfr1–Swi5 complex stabilize the presynaptic filament. Further studies will be required to determine whether these factors stabilize the presynaptic filament by inducing a conformational change that stabilizes ATP bound within the ATP binding pocket of hDMC1.

Supplementary Material

Refer to Web version on PubMed Central for supplementary material.

Acknowledgments

This work was supported in part by HHMI grant #52005867 awarded to Clemson University from the Howard Hughes Medical Institute through the Precollege and Undergraduate Science Education Program (AJH) and National Institutes of Health grant GM098510 (MGS). We thank Leigh Anne Clark for helpful comments on the manuscript.

References

1. Keeney S, Giroux CN, Kleckner N. Meiosis-specific DNA double-strand breaks are catalyzed by Spo11, a member of a widely conserved protein family. Cell. 1997; 88:375–384. [PubMed: 9039264]
2. Ogawa T, Yu X, Shinohara A, Egelman EH. Similarity of the yeast RAD51 filament to the bacterial RecA filament. Science. 1993; 259:1896–1899. [PubMed: 8456314]
3. Conway AB, Lynch TW, Zhang Y, Fortin GS, Fung CW, Symington LS, Rice PA. Crystal structure of a Rad51 filament. Nat Struct Mol Biol. 2004; 11:791–796. [PubMed: 15235592]
4. Sheridan SD, Yu X, Roth R, Heuser JE, Sehorn MG, Sung P, Egelman EH, Bishop DK. A comparative analysis of DMC1 and Rad51 nucleoprotein filaments. Nucleic Acids Res. 2008; 36:4057–4066. [PubMed: 18535008]
5. Sehorn MG, Sigurdsson S, Bussen W, Unger VM, Sung P. Human meiotic recombinase DMC1 promotes ATP-dependent homologous DNA strand exchange. Nature. 2004; 429:433–437. [PubMed: 15164066]
6. Sung P. Catalysis of ATP-dependent homologous DNA pairing and strand exchange by yeast RAD51 protein. Science. 1994; 265:1241–1243. [PubMed: 8066464]
7. Krejci L, Altmannova V, Spirek M, Zhao X. Homologous recombination and its regulation. Nucleic Acids Res. 2012; 40:5795–5818. [PubMed: 22467216]
8. Phadnis N, Hyppa RW, Smith GR. New and old ways to control meiotic recombination. Trends Genet. 2011; 27:411–421. [PubMed: 21782271]
9. Lim DS, Hasty P. A mutation in mouse rad51 results in an early embryonic lethal that is suppressed by a mutation in p53. Mol Cell Biol. 1996; 16:7133–7143. [PubMed: 8943369]
10. Tsuzuki T, Fujii Y, Sakumi K, Tominaga Y, Nakao K, Sekiguchi M, Matsushiro A, Yoshimura Y, Morita T. Targeted disruption of the Rad51 gene leads to lethality in embryonic mice. Proc Natl Acad Sci U S A. 1996; 93:6236–6240. [PubMed: 8692798]
11. Pittman DL, Cobb J, Schimenti KJ, Wilson LA, Cooper DM, Brignull E, Handel MA, Schimenti JC. Meiotic prophase arrest with failure of chromosome synapsis in mice deficient for DMC1, a germline-specific RecA homolog. Mol Cell. 1998; 1:697–705. [PubMed: 9660953]
12. Bugreev DV, Golub EI, Stasiak AZ, Stasiak A, Mazin AV. Activation of human meiosis-specific recombinase DMC1 by Ca^{2+} J Biol Chem. 2005; 280:26886–26895. [PubMed: 15917244]
13. Baumann P, Benson FE, West SC. Human Rad51 protein promotes ATP-dependent homologous pairing and strand transfer reactions in vitro. Cell. 1996; 87:757–766. [PubMed: 8929543]
14. Sigurdsson S, Trujillo K, Song B, Stratton S, Sung P. Basis for avid homologous DNA strand exchange by human Rad51 and RPA. J Biol Chem. 2001; 276:8798–8806. [PubMed: 11124265]
15. Bugreev DV, Mazin AV. Ca^{2+} activates human homologous recombination protein Rad51 by modulating its ATPase activity. Proc Natl Acad Sci U S A. 2004; 101:9988–9993. [PubMed: 15226506]
16. Bugreev DV, Pezza RJ, Mazina OM, Voloshin ON, Camerini-Otero RD, Mazin AV. The resistance of DMC1 D-loops to dissociation may account for the DMC1 requirement in meiosis. Nat Struct Mol Biol. 2011; 18:56–60. [PubMed: 21151113]
17. Bugreev DV, Hanaoka F, Mazin AV. Rad54 dissociates homologous recombination intermediates by branch migration. Nat Struct Mol Biol. 2007; 14:746–753. [PubMed: 17660833]
18. Bishop DK, Park D, Xu L, Kleckner N. DMC1: a meiosis-specific yeast homolog of *E. coli* recA required for recombination, synaptonemal complex formation, and cell cycle progression. Cell. 1992; 69:439–456. [PubMed: 1581960]

19. Shinohara A, Ogawa H, Ogawa T. Rad51 protein involved in repair and recombination in *S. cerevisiae* is a RecA-like protein. Cell. 1992; 69:457–470. [PubMed: 1581961]
20. Story RM, Steitz TA. Structure of the recA protein-ADP complex. Nature. 1992; 355:374–376. [PubMed: 1731253]
21. Rehrauer WM, Kowalczykowski SC. The DNA binding site(s) of the *Escherichia coli* RecA protein. J Biol Chem. 1996; 271:11996–12002. [PubMed: 8662640]
22. VanLoock MS, Yu X, Yang S, Lai AL, Low C, Campbell MJ, Egelman EH. ATP-mediated conformational changes in the RecA filament. Structure. 2003; 11:187–196. [PubMed: 12575938]
23. Jain SK, Cox MM, Inman RB. On the role of ATP hydrolysis in RecA protein-mediated DNA strand exchange. III. Unidirectional branch migration and extensive hybrid DNA formation. J Biol Chem. 1994; 269:20653–20661. [PubMed: 8051165]
24. Chi P, Van Komen S, Sehorn MG, Sigurdsson S, Sung P. Roles of ATP binding and ATP hydrolysis in human Rad51 recombinase function. DNA Repair (Amst). 2006; 5:381–391. [PubMed: 16388992]
25. Say AF, Ledford LL, Sharma D, Singh AK, Leung WK, Sehorn HA, Tsubouchi H, Sung P, Sehorn MG. The budding yeast Mei5–Sae3 complex interacts with Rad51 and preferentially binds a DNA fork structure. DNA Repair (Amst). 2011; 10:586–594. [PubMed: 21543267]
26. Sung P, Higgins D, Prakash L, Prakash S. Mutation of lysine-48 to arginine in the yeast RAD3 protein abolishes its ATPase and DNA helicase activities but not the ability to bind ATP. EMBO J. 1988; 7:3263–3269. [PubMed: 2846277]
27. Rehrauer WM, Kowalczykowski SC. Alteration of the nucleoside triphosphate (NTP) catalytic domain within *Escherichia coli* recA protein attenuates NTP hydrolysis but not joint molecule formation. J Biol Chem. 1993; 268:1292–1297. [PubMed: 8419331]
28. Shan Q, Cox MM, Inman RB. DNA strand exchange promoted by RecA K72R. Two reaction phases with different Mg^{2+} requirements. J Biol Chem. 1996; 271:5712–5724. [PubMed: 8621437]
29. Petukhova G, Stratton S, Sung P. Catalysis of homologous DNA pairing by yeast Rad51 and Rad54 proteins. Nature. 1998; 393:91–94. [PubMed: 9590697]
30. Li Z, Golub EI, Gupta R, Radding CM. Recombination activities of HsDmc1 protein, the meiotic human homolog of RecA protein. Proc Natl Acad Sci U S A. 1997; 94:11221–11226. [PubMed: 9326590]
31. Hong EL, Shinohara A, Bishop DK. Saccharomyces cerevisiae Dmc1 protein promotes renaturation of single-strand DNA (ssDNA) and assimilation of ssDNA into homologous super-coiled duplex DNA. J Biol Chem. 2001; 276:41906–41912. [PubMed: 11551925]
32. De Zutter JK, Knight KL. The hRad51 and RecA proteins show significant differences in cooperative binding to single-stranded DNA. J Mol Biol. 1999; 293:769–780. [PubMed: 10543966]
33. Passy SI, Yu X, Li Z, Radding CM, Masson JY, West SC, Egelman EH. Human Dmc1 protein binds DNA as an octameric ring. Proc Natl Acad Sci U S A. 1999; 96:10684–10688. [PubMed: 10485886]
34. Chow SA, Honigberg SM, Bainton RJ, Radding CM. Patterns of nuclease protection during strand exchange. recA protein forms heteroduplex DNA by binding to strands of the same polarity. J Biol Chem. 1986; 261:6961–6971. [PubMed: 3009481]
35. Petukhova G, Van Komen S, Vergano S, Klein H, Sung P. Yeast Rad54 promotes Rad51-dependent homologous DNA pairing via ATP hydrolysisdriven change in DNA double helix conformation. J Biol Chem. 1999; 274:29453–29462. [PubMed: 10506208]
36. Gupta RC, Golub E, Bi B, Radding CM. The synaptic activity of HsDmc1, a human recombination protein specific to meiosis. Proc Natl Acad Sci U S A. 2001; 98:8433–8439. [PubMed: 11459986]
37. Brenner SL, Mitchell RS, Morrical SW, Neuendorf SK, Schutte BC, Cox MM. recA protein-promoted ATP hydrolysis occurs throughout recA nucleoprotein filaments. J Biol Chem. 1987; 262:4011–4016. [PubMed: 2951381]
38. Bianco PR, Weinstock GM. Interaction of the RecA protein of *Escherichia coli* with single-stranded oligodeoxyribonucleotides. Nucleic Acids Res. 1996; 24:4933–4939. [PubMed: 9016663]

39. Sung P, Stratton SA. Yeast Rad51 recombinase mediates polar DNA strand exchange in the absence of ATP hydrolysis. J Biol Chem. 1996; 271:27983–27986. [PubMed: 8910403]

40. Okorokov AL, Chaban YL, Bugreev DV, Hodgkinson J, Mazin AV, Orlova EV. Structure of the hDmc1-ssDNA filament reveals the principles of its architecture. PLoS ONE. 2010; 5:e8586. [PubMed: 20062530]

41. Kinebuchi T, Kagawa W, Enomoto R, Tanaka K, Miyagawa K, Shibata T, Kurumizaka H, Yokoyama S. Structural basis for octameric ring formation and DNA interaction of the human homologous-pairing protein Dmc1. Mol Cell. 2004; 14:363–374. [PubMed: 15125839]

42. Kumar KA, Mahalakshmi S, Muniyappa K. DNA-induced conformational changes in RecA protein. Evidence for structural heterogeneity among nucleoprotein filaments and implications for homologous pairing. J Biol Chem. 1993; 268:26162–26170. [PubMed: 8253735]

Abbreviations

HR	homologous recombination
hDMC1	human DMC1
hRAD51	human RAD51
ss	single-stranded
ds	double-stranded
NTA	nitrilotriacetic acid
BSA	bovine serum albumin
SDS-PAGE	sodium dodecyl sulfate polyacrylamide gel electrophoresis

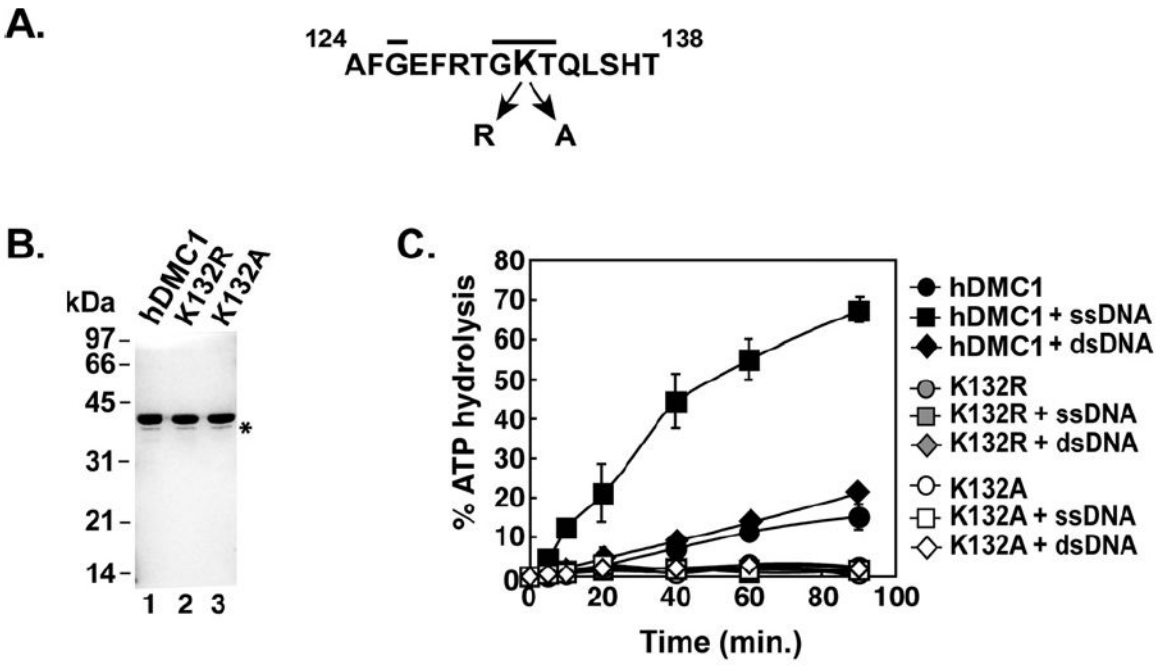

Fig. 1.

Purification and ATP hydrolysis activity of wild type and Walker A variants of hDMC1. (A) hDMC1 Walker A motif consisting of amino acid residues 124–138. The bars depict the conserved residues of the Walker A motif. The conserved lysine at position 132 (K) residue was substituted with either arginine (R) or alanine (A). (B) Purified $hDMC1_{WT}$ (hDMC1; lane 1), $hDMC1_{K132R}$ (K132R; lane 2), and $hDMC1_{K132A}$ (K132A; lane 3) 1.5 μg each variant was resolved on 12% SDS-PAGE polyacrylamide gel stained with Coomassie Blue. * Denotes a C-terminal truncation of hDMC1. (C) Determination of ATP hydrolysis activity of hDMC1 and walker A motif variants. Purified $hDMC1_{WT}$ (hDMC1), $hDMC1_{K132R}$ (K132R), and $hDMC1_{K132A}$ (K132A) were incubated with [γ-^{32}P] ATP in the presence or absence of ϕX174 (+) virion single strand (ssDNA) or ϕX174 replicative form I (dsDNA). The samples were withdrawn at the indicated time points and subjected to thin layer chromatography (TLC) followed by phosphorimager analysis.

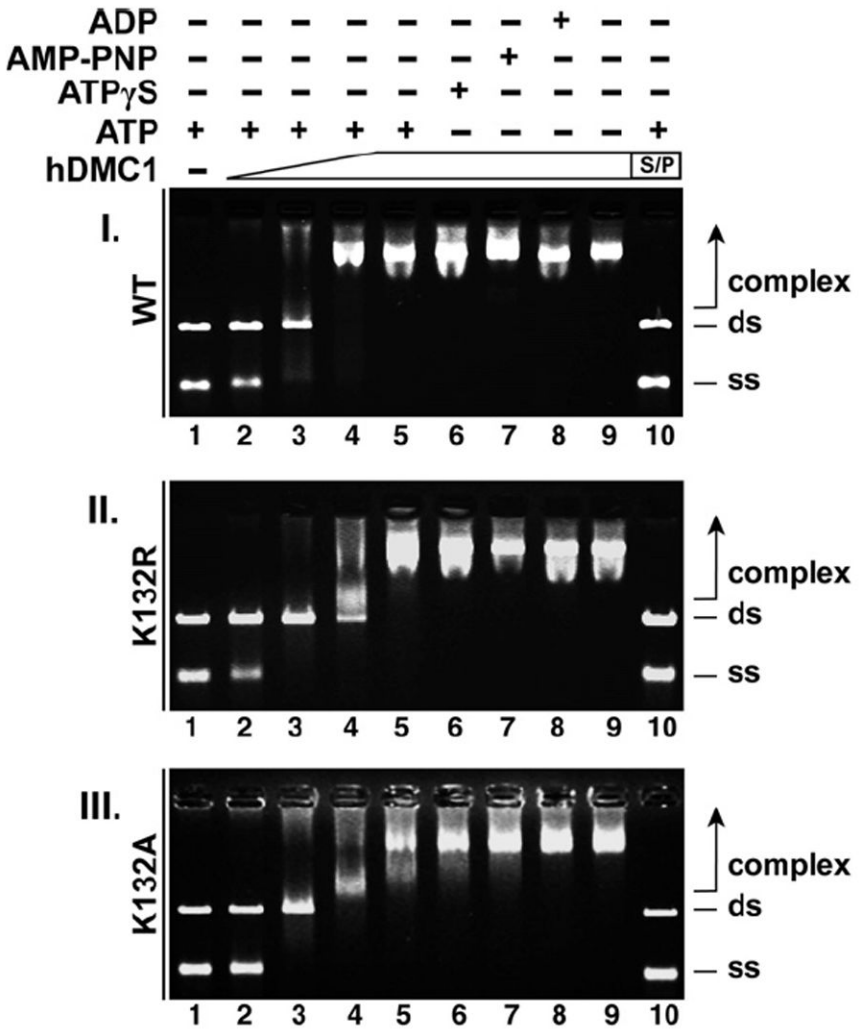

Fig. 2.

DNA binding activity of wild type and Walker A variants of hDMC1. (panel I) $hDMC1_{WT}$ (1.4 μM, lane 2; 2.8 μM, lane 3; 5.6 μM, lane 4; 11.2 μM, lanes 5–11) was incubated with ϕX174 (+) ssDNA DNA (ss) and linearized ϕX174 RF (I) dsDNA (ds) in the absence (lane 9) or presence of ATP (lanes 1–5 and 10) and nucleotide analogs (ATP-γ-S, lane 6; AMP–PNP, lane 7; and ADP, lane 8). The reaction products were analyzed on 1% agarose gels. Lane 11, the reaction was deproteinized prior loading on the agarose gel. The $hDMC1_{K132R}$ (panel II) and $hDMC1_{K132A}$ (panel III) were analyzed as described for $hDMC1_{WT}$.

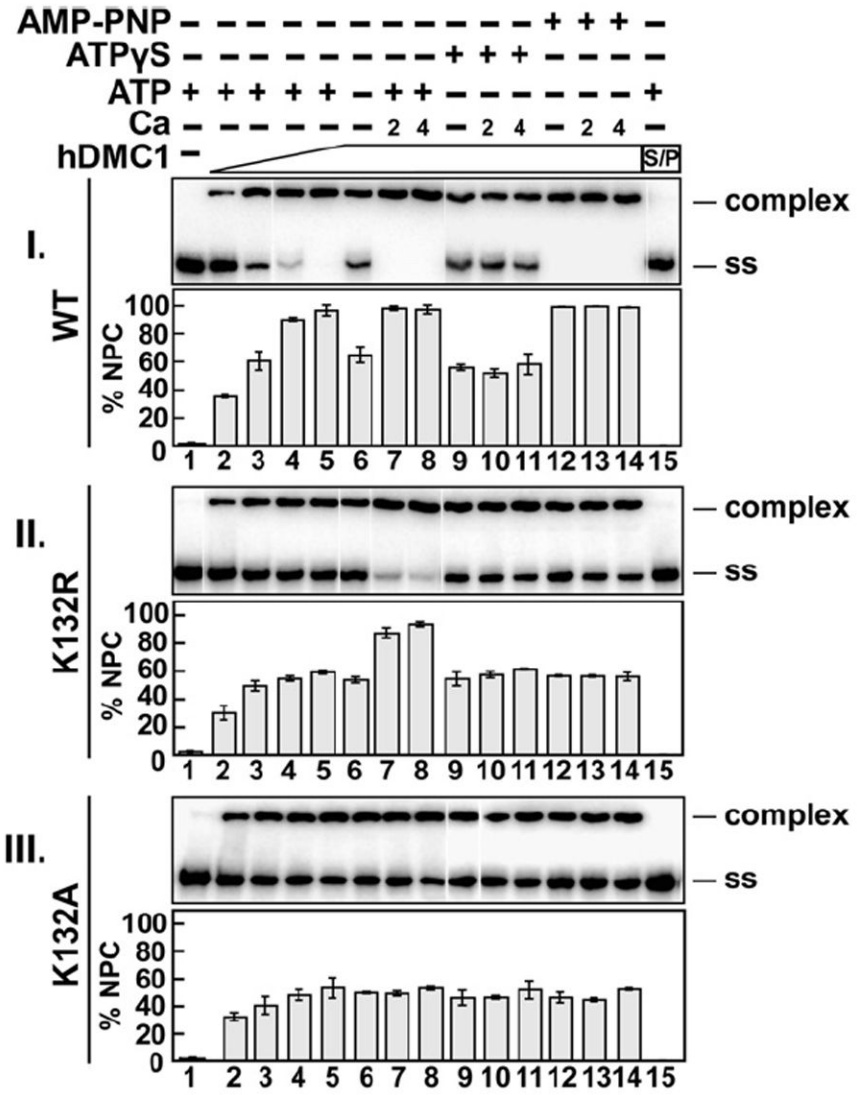

Fig. 3.

Oligonucleotide DNA binding of wild type and Walker A variants of hDMC1. (panel I) $hDMC1_{WT}$ (0.25 μM, lane 2; 0.7 μM, lane 3; 1.4 μM, lane 4; 2.8 μM, lanes 5–15) was incubated with ^{32}P-labeled OL90 ssDNA (ss) in the absence (lane 6) or presence of ATP (lanes 1–5, 7–8, and 15), ATP-γ-S (lanes 9–11), AMP–PNP, (lanes 12–14) and Ca^{2+} (2 mM, lanes 7, 10 and 13; 4 mM, lanes 8, 11 and 14). The reaction products were resolved on non-denaturing 10% polyacrylamide gels. The $hDMC1_{K132R}$ (panel II) and $hDMC1_{K132A}$ (panel III) were analyzed as described for $hDMC1_{WT}$.

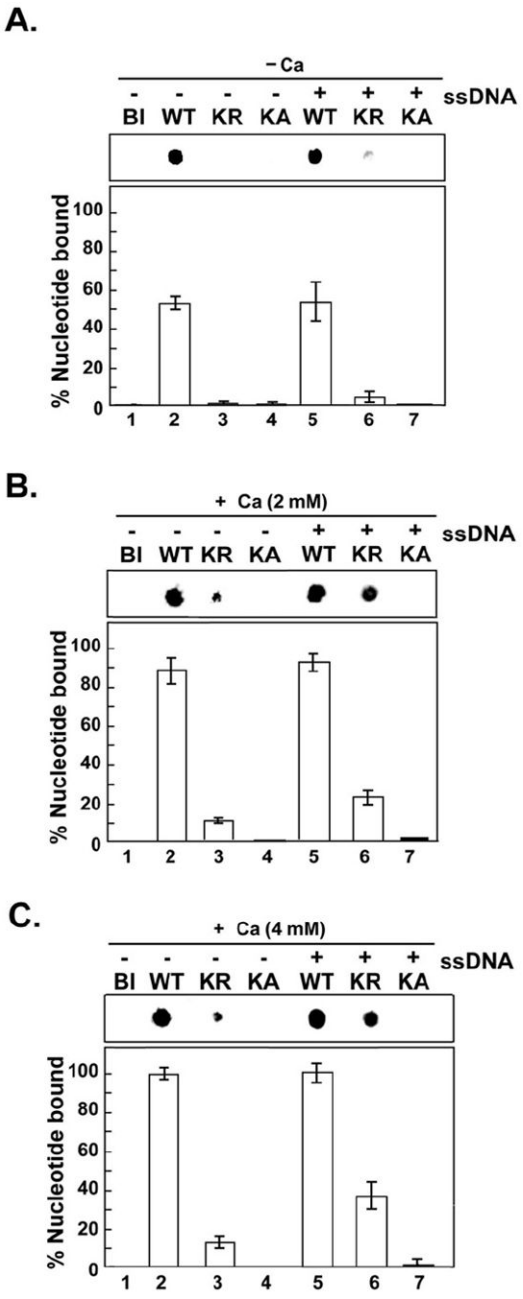

Fig. 4.

Nucleotide binding by wild type and Walker A variants of hDMC1. (A) $hDMC1_{WT}$ (lane 2 and 5), $hDMC1_{K132R}$ (lane 3 and 6) and $hDMC1_{K132A}$ (lane 4 and 7) were incubated with [α-^{32}] ATP in the absence (lanes 1–4) or presence of ϕX174 (+) strand (ssDNA) (lanes 5–7) either in the absence (A) or presence of 2 mM Ca^{2+} (B) or 4 mM Ca^{2+} (C). The reaction products were subjected to dot filtration through a nylon membrane in a mini-fold apparatus followed by immediate washes with reaction buffer. The relative amount of bound nucleotide was quantified using a phosphorimager.

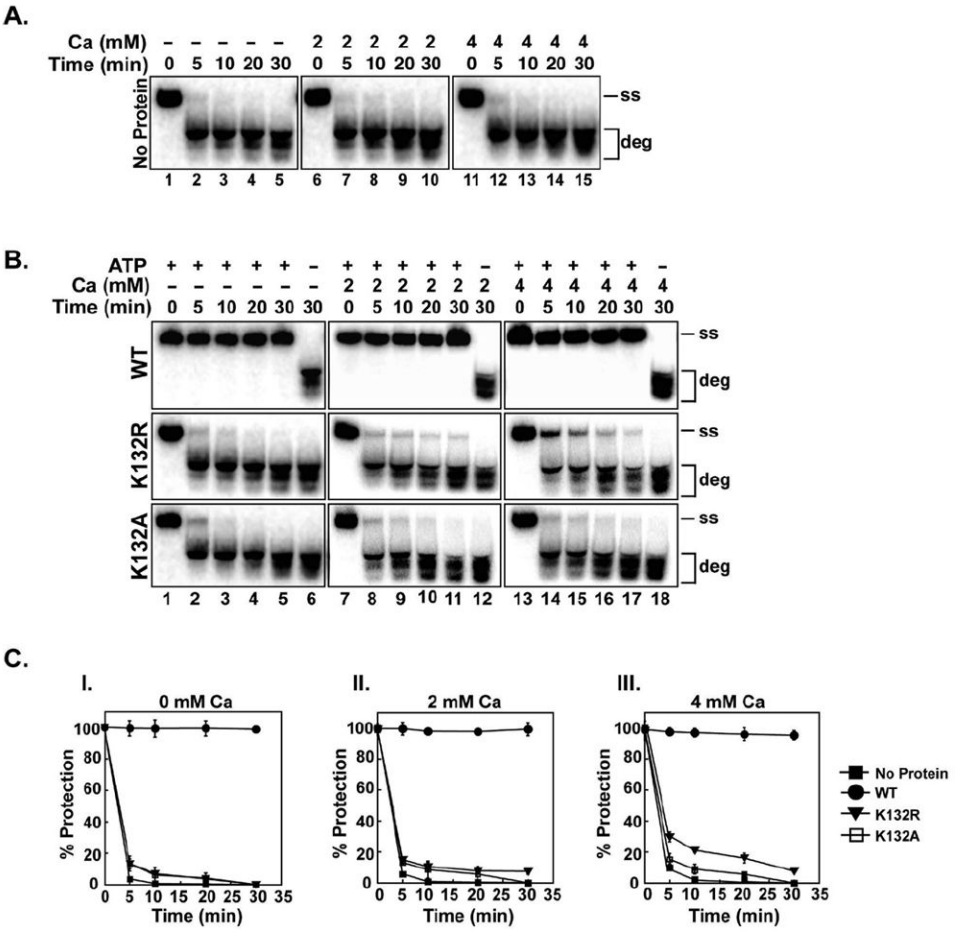

Fig. 5.

Protection of ssDNA by presynaptic filaments formed by wild type and Walker A variants of hDMC1. (A) ^{32}P-labeled OL90 ssDNA was incubated in the absence of hDMC1 with ATP in the absence (lanes 1–5) or presence of Ca^{2+} (2 mM, lanes 6–10; or 4 mM, lanes 11–15) for 10 min followed by DNase I digestion. Reaction products were withdrawn at indicated time points, deproteinized and resolved on non-denaturing 10% polyacrylamide gels. (B) ^{32}P-labeled OL90 ssDNA was incubated with $hDMC1_{WT}$ (WT), $hDMC1_{K132R}$ (K132R) or $hDMC1_{K132A}$ (K132A) in the absence (lane 6, 12, and 18) or presence of ATP (lanes 1–5, 7–11, and 13–17) in the absence (lanes 1–6) or presence of Ca^{2+} (2 mM, lanes 7–12; or 4 mM, lanes 13–18) for 10 min followed by DNase I digestion. The reaction products were analyzed as described in (A). (C) The data presented in (A) and (B) were plotted.

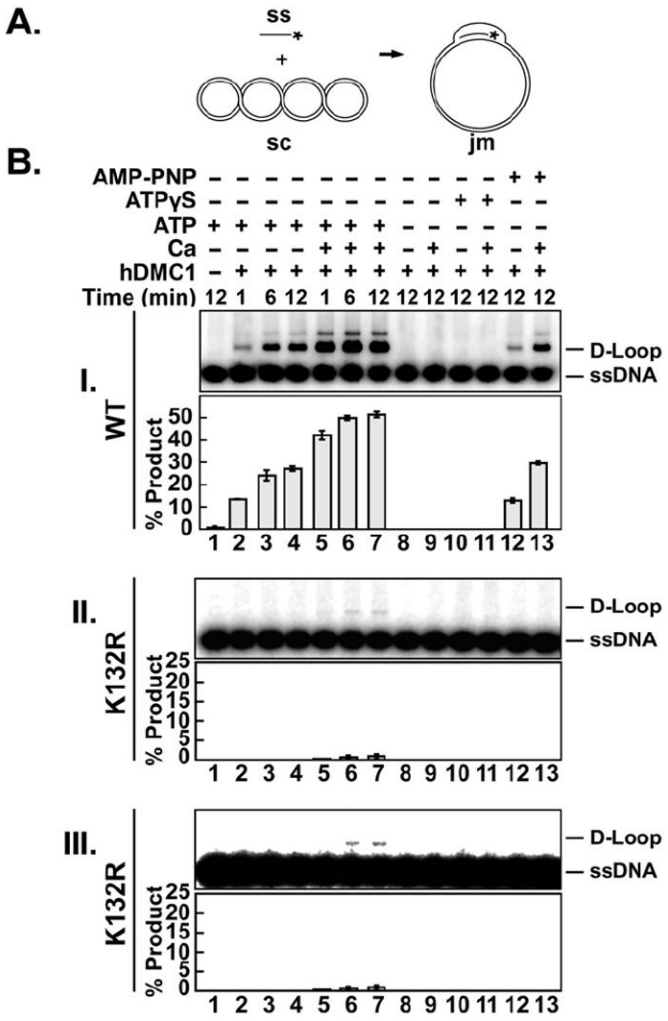

Fig. 6.

Dependence of ATP hydrolysis for Displacement loop (D-loop) formation. (A) Reaction scheme. ss, ssDNA; sc, super-coiled DNA; jm, joint molecule. The asterisks represent the ^{32}P label. (B) $hDMC1_{WT}$ (panel I, WT) and $hDMC1_{K132R}$ (panel II, K132R) was incubated with ^{32}P labeled OL90 ssDNA in the absence (lanes 8–9) or presence of ATP (lanes 1–7), ATP analogs (ATP-γ-S, lanes 10–11; AMP–PNP, lanes 12–13) and in the absence (lanes 1–4, 8, 10, and 12) presence of 2 mM Ca^{2+} (panel I, lanes 5–7, 9, 11, and 13) or 4 mM Ca^{2+} (panel II and III, lanes 5–7, 9, 11, and 13). The reaction was initiated with the addition of super-coiled DNA. Samples were withdrawn at the indicated time points, deproteinized and the reaction products were analyzed on a 1% agarose gel. The gel in panel II was overexposed (panel III). The results from three replicates were graphed for each hDMC1 variant.

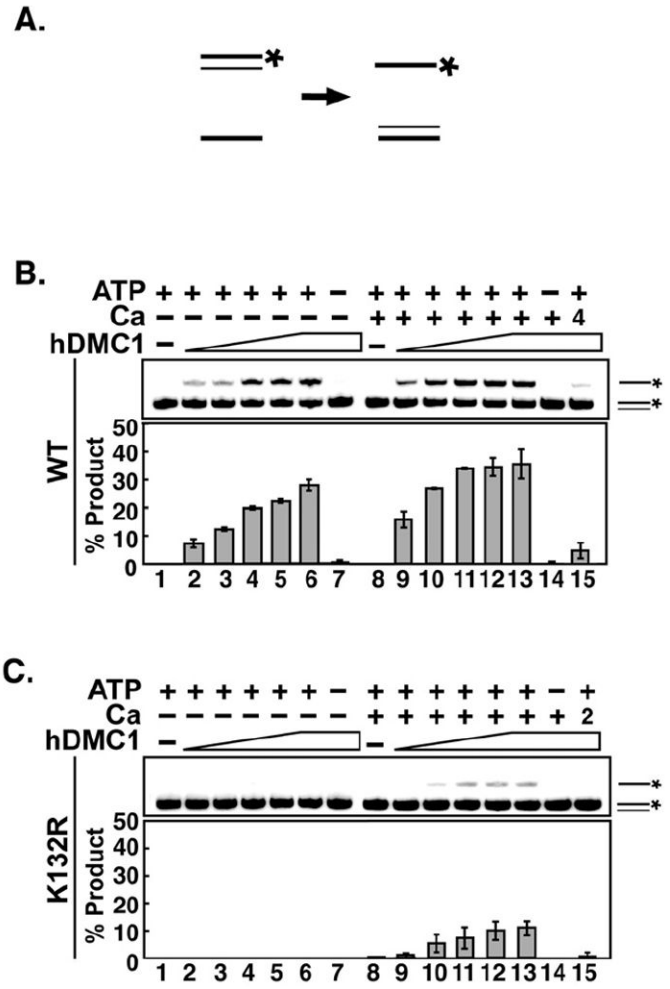

Fig. 7.

Dependence of ATP hydrolysis for homologous DNA pairing and strand exchange. (A) Reaction scheme. The asterisks represent the ^{32}P label. (B) hDMC1$_{WT}$ or (C) hDMC1$_{K132R}$ (0.25 μM, lanes 2 and 9; 0.5 μM, lanes 3 and 10; 1.0 μM, lanes 4 and 11; 2.0 μM, lanes 5 and 12; 3.0 μM, lanes 6–7 and 13–15) was incubated with OL83 oligonucleotide substrate in the absence (lanes 7 and 14) or presence of ATP (lanes 1–6, 8–13, and 15) in the absence (lanes 1–7) or presence of Ca^{2+} (2 mM, lanes 8–14; 4 mM, lane 15) followed by the addition of ^{32}P-labeled dsDNA. The reactions were further incubated followed by deproteinization and resolved on a 12% non-denaturing polyacrylamide gel. The graph represents the data from three replicates of the experiment.

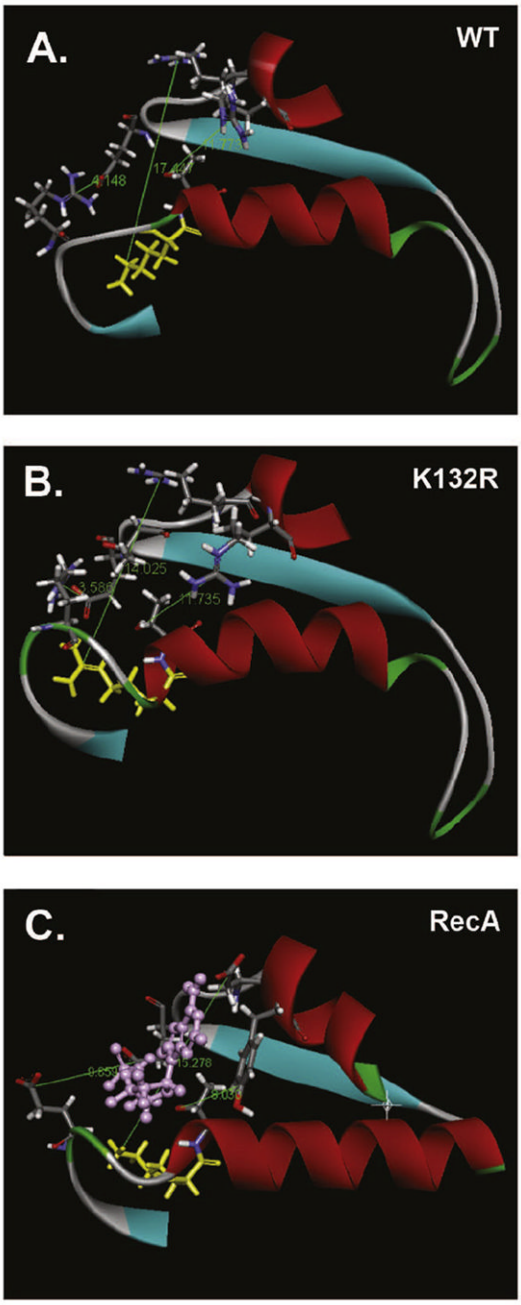

Fig. 8.

Molecular modeling and energy minimization of $hDMC1_{K132R}$. (A) In $hDMC1_{WT}$, the atom pairs and distances that span the putative nucleotide-binding site were: K132:NZ-R166:CZ (17.447 Å); T133:OG1-R169:CZ (11.773 Å); R129:CZ-E162: CD (4.148 Å), and (B) In $hDMC1_{K132R}$, these distances were R132:CZ-R166:CZ (14.025 Å); T133:OG1-R169:CZ (11.735 Å); R129:CZ-E162:CD (3.598 Å). The hDMC1 residues are based on their counterparts in the RecA protein (C) with corresponding atom pairs and distances: K72:NZ-D100:CG (15.278 Å); T73:OG1-Y103:CZ (8.030 Å); and E68:CD-E96:CD (9.859 Å). For comparison, the original distances in $hDMC1_{WT}$ prior to minimization were: 16.822 Å for

K132:NZ-R166:CZ, 10.560 Å for T133:OG1-R169:CZ, and 9.413 Å for R129:CZ-E162:CD.